Understanding marine dune dynamics in a shallow shelf sea using sediment mobility indices

N. Durand *France Energies Marines, Plouzané, France – noemie.durand@ite-fem.org*
P. Tassi *EDF Recherche & Développement, Chatou, France – pablo.tassi@edf.fr*
O. Blanpain *France Energies Marines, Plouzané, France – olivier.blanpain@ite-fem.org*
A. Lefebvre *MARUM, University of Bremen, Germany – alefebvre@marum.de*

ABSTRACT: Tides, winds, and waves shape the seabed of shallow shelf seas. In sandy, energetic environments, marine dunes can develop. The scale and dynamic behaviour of these bed forms warrant some interest, for example related to the interactions with human activities (mining, renewable energies). Yet, the morphology and dynamics of dunes are still poorly understood in open marine environments. A complex process-based model (http://www.opentelemac.org) is being developed for an application in the southern North Sea, offshore of Dunkirk in France, with the objective to improve our comprehension of the processes at play.

1 INTRODUCTION

Marine dunes are large, flow-transverse bed forms with height of 1 m to 5 m and wavelength of the order of hundreds of metres (Ashley 1990). They develop almost exclusively on sandy seabeds, in settings where bedload is the predominant mechanism of sediment transport. They are very dynamic sedimentary structures that grow, evolve and migrate in space and time, at rates of up to tens of metres per year.

A complex process-based numerical model (accounting for the interactions between currents, waves and sediment transport processes) is being developed for an application offshore of Dunkirk, on the northern coast of France, close to the Belgium border. Marine dunes coexist there with sand banks. The site is subjected to relatively strong tidal flows, and waves originating from the Atlantic Ocean and the North Sea.

The combined influence of waves and currents is expected to mobilise the sediments on the seabed. As a first step, outputs from the calibrated hydrodynamic and wave models are used to construct sediment mobility maps that highlight some of the processes at play in this complex and highly dynamic environment.

2 STUDY AREA

This study focuses on the southern North Sea, offshore of Dunkirk (Figure 1). Seabed levels in the area are generally between 7 and 30 m below mean sea level (MSL), noting the presence of offshore sand banks with crests as high as -6 m MSL. The seabed sediment consists of well sorted medium sands with d_{50} grain sizes between 240 and 450 µm based on recent samples. It is not expected that sediments exhibit cohesive properties.

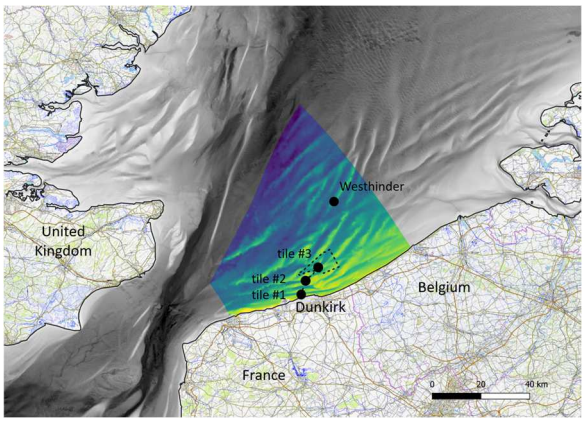

Figure 1. Location map showing the full model extent (in colour), the proposed offshore wind farm footprint (dashed line) and the survey tiles (filled circles) (Source of the background data: Shom 2015 and https://opentopomap.org/).

The region is characterised by a macro-tidal regime (ca. 5.5 m spring tidal range, 3.3 m neap tidal range). The tide is asymmetric: it rises faster than it falls. This asymmetry is also observed in the tidal currents and the flood, trending North-East, is generally stronger than the ebb, trending South-West (ca. 1.25 m/s compared to 0.75 m/s).

While the offshore wave climate (at Westhinder, Figure 1) is dominated by south-westerly waves, some significant events from the North-West to the North-East are noted. 56% of the waves are under 1 m. The wave condition with a 1-year return period is estimated at H_s = 4.4 m, with associated mean period, T_z, around 7 s.

3 METHODS

3.1 Metocean and bathymetric surveys

A large metocean and bathymetric data set has been collected in support of Dunkirk offshore wind farm project and for research purposes. Site-specific meteorological and hydrodynamic campaigns have been carried out for periods of up to six months. Long-term metocean observations are also available from the Flanders Marine Institute (VLIZ) at Westhinder measurement pile / buoy. All these records inform the wind velocity, atmospheric pressure, water level, current velocity (at various elevations in the water column), and wave conditions. They provide a valuable in-situ data set against which to calibrate the hydrodynamic and wave models.

Recurrent and detailed bathymetric surveys have been carried out. Two large-area surveys covering the wind farm footprint (dashed outline in Figure 1) were conducted in 2016-2017 (Shom) and in June 2021 (EMD). Separately, eight surveys were performed between 2019 and 2021 (FEM), in three pre-defined tiles (filled circles in Figure 1) selected to include a variety of bed forms. These local-area surveys will serve to calibrate the morphodynamic model. A special emphasis is placed on tile #1 (in the navigation approach channel) going forward. Bed levels surveyed in November 2019 are reproduced in Figure 2.

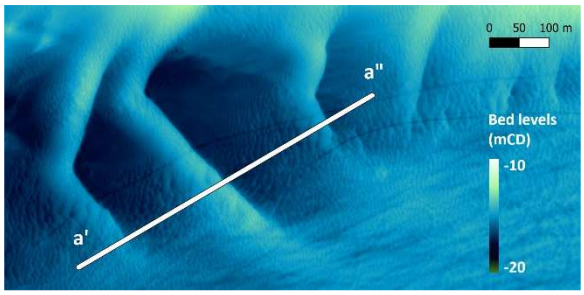

Figure 2. Bed levels in tile #1 in November 2019 (FEM) showing section a'-a" where dune profiles have been extracted.

3.2 Coastal area model

Both 2D and 3D coastal area models are being developed based on the open source TELEMAC system (www.opentelemac.org). These models consider interactions between tidal flows, winds, waves and sediment transport processes. The same computational domain and spatial discretisation are used throughout.

The domain extends from Calais to Ostend in Belgium, for approximately 80 km. Its offshore extent varies between 15 km in the Dover Strait and 75 km in the East (Figure 1). An unstructured finite element mesh with spatially varying resolution is used. The size of the triangular elements varies gradually from 10 m in the areas of interest to a maximum of 3000 m away from them. Overall, the computational domain comprises approximately 64 k nodes.

Digital elevation models of the seabed throughout the model area have been constructed that are relevant to different time periods.

3.3 Hydrodynamic model

The open source TELEMAC system has both 2-dimensional (2D) and 3-dimensional (3D) hydrodynamic modules. While TELEMAC-2D solves the depth-integrated shallow water equations, TELEMAC-3D solves the 3D Navier-Stokes equations with, or without, the hydrostatic pressure assumption (Hervouet 2007). Both modules were used in this study, and if the model validation is presented for the 3D module in section 3.5, subsequent mobility maps and analysis are largely based on depth-averaged results. In

the 2D model, the bottom roughness is parameterised with the Chézy formulation, spatially constant coefficient of 65 $m^{½}/s$. This value is appropriate for sandy seabeds. In the 3D model, a Nikuradse roughness of 862.5 µm is used, corresponding to 2.5 times the grain size representative of the study area.

Time-varying sea levels are applied along the open water boundaries of the hydrodynamic model. These time histories are computed from the 34 constituents available from the FES2014 database produced by Noveltis, Legos and CLS (https://www.aviso.altimetry.fr) at a spatial resolution of 1/16°. In addition to tidal forcing, time- and space-varying wind and pressure fields are applied over the model area to account for the effect of a wind blowing on the water surface and causing set-up and wind-induced currents, as well as the "inverted barometer" effect, caused by atmospheric pressure variations. These fields were extracted from the Météo-France short-term operational forecast AROME (Boutier 2007) at a spatial resolution of 1/40° and hourly intervals, after it was demonstrated that its higher resolution outweighed the reputedly lower accuracy of forecast models in the study area (Durand et al. 2022b).

3.4 Wave model

The wave generation and transformation module, TOMAWAC, solves the spectral action density balance equation with sources and sinks, and no a priori restrictions on the spectral shape or evolution (Benoit et al. 1996).

Time-varying wave spectra were obtained from the ANEMOC-3 sea state hindcast database (Raoult et al. 2018 and Teles et al. 2022) at 56 locations along the open boundaries of the wave model. The use of spectral data is preferred over integrated sea states, in that it reduces the loss of information between the global database and the local model. The spectra are discretised with 32 frequencies and 36 directions and output at half-hourly intervals. AROME time- and space-varying wind fields are applied over the model area to account for local wave generation due to winds. In shallow shelf seas, tidal effects also play a role on wave propagation and transformation. These effects are considered by using time- and space-varying maps of water depths and currents obtained from the validated hydrodynamic model of the same area.

3.5 Model calibration and validation

Durand et al. (2022a) details the procedure for the calibration and validation of the hydrodynamic model against in-situ free surface elevation and depth-averaged flow velocity data. Table 1 and Figure 3 present updated results.

Table 1: Performance of the hydrodynamic model against observed data for a complete spring-neap cycle. Root Mean Square Error (RMSE) values and Relative Mean Absolute Error (RMAE) in brackets

	tidal levels	current speeds
Site 1	--	0.13 m/s (19%)
Site 2	--	0.09 m/s (15%)
Site 3	0.26 m (5%)	0.11 m/s (17%)
Site 5	0.15 m (3%)	0.12 m/s (14%)
Site 7	--	0.09 m/s (13%)
Westhinder '16	0.18 m (3%)	--
Westhinder '21	0.15 m (3%)	--

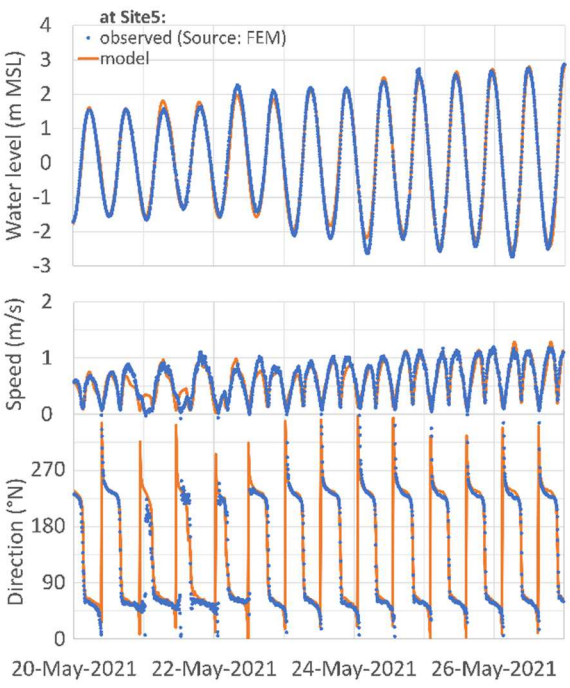

Figure 3. Comparison of model predictions against observed tidal levels (top), current magnitude (centre) and direction (bottom) for a 7-day period in 2021.

Durand et al. (2022b) presents the calibration and validation of the wave model against in-situ wave conditions (significant height, mean period and mean direction). These results are reproduced in Table 2 and Figure 4.

Table 2: Performance of the wave model against observed data (40 days in 2016, 16 days in 2021). RMSE values and RMAE in brackets

	Hm_0	Tm_{02}
Site 1	0.13 m (18%)	0.5 s (16%)
Site 2	0.15 m (15%)	0.4 s (10%)
Site 7	0.16 m (20%)	0.6 s (13%)
Westhinder '16	0.18 m (15%)	0.6 s (14%)
Westhinder '21	0.18 m (18%)	0.6 s (12%)
Gravelines	0.16 m (22%)	0.8 s (16%)

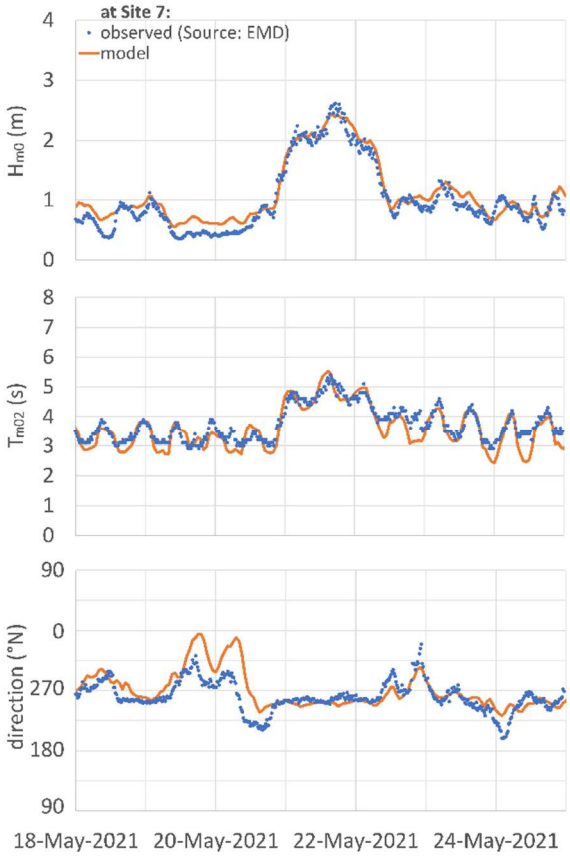

Figure 4. Comparison of model predictions against observed wave height Hm_0 (top), mean wave period Tm_{02} (centre), and mean wave direction (bottom) for a 7-day period in 2021.

Sutherland et al. (2004) propose a statistical approach based on RMAE, and associated classification, to evaluate the performance of numerical models. It follows that the hydrodynamic model results (tidal level and current magnitude) fall in the "excellent" category (RMAE < 20%) at all six validation sites. A similar conclusion is drawn for the wave model results at all but two sites where the performance is qualified as "good" (RMAE < 40%).

Calibrated numerical models can be used to overcome spatial and temporal limitations in field observations. And so a two-year period (January 2020 to December 2021) was run in the validated hydrodynamic and wave models to perform some preliminary analysis of sediment mobility in the study area, based on oceanographic considerations.

3.6 Bed shear-stress

Grain shear-stresses induced by currents and those induced by waves are computed independently by the coupled hydrodynamic and wave models. The shear-stresses generated by currents alone, τ_C, are computed from the water density ρ = 1027 kg/m^3, the dimensionless drag coefficient C_D (a function of the friction coefficient) and the depth-averaged current velocity U as a first approximation:

$$\tau_C = \rho C_D U^2 \quad (1)$$

The shear-stresses generated by waves alone, τ_W, are computed from the water density, the rms orbital velocity near the seabed U_{rms} (small-amplitude linear wave theory, in the absence of a current), and the dimensionless wave friction factor f_w defined in Swart (1976):

$$\tau_W = \rho f_w U_{rms}^2 \quad (2)$$

The mean and maximum bed shear-stresses during a wave cycle, due to the combined action of waves and currents, are computed from Soulsby (1997):

$$\tau_m = \tau_C \left[1 + 1.2 \left(\frac{\tau_W}{\tau_C + \tau_W}\right)^{3.2}\right] \quad (3)$$

$$\tau_{max} = \sqrt{(\tau_m + \tau_W \cos\phi)^2 + (\tau_W \sin\phi)^2} \quad (4)$$

where ϕ = angle between the current and wave directions.

3.7 Sediment mobilisation

To estimate sediment mobilisation, the threshold bed shear-stress for the onset of motion is computed for a sediment with median grain diameter d_{50} of 345 µm (corresponding to the average sample):

$$\tau_{cr} = \theta_{cr} \left[g \left(\rho_s - \rho \right) d_{50} \right] \quad (5)$$

where g = 9.81 m/s^2 is the acceleration due to gravity; ρ_S = 2650 kg/m^3 is the sediment density; and θ_{cr} is the threshold Shields parameter estimated from Soulsby (1997).

Seabed sediment is mobilised by either current, wave, or the combined wave and current action. The dominant processes will vary in space and in time. Their relative importance can be estimated from the percentage of time when the threshold bed shear-stress, τ_{cr} (Eq. 5), is exceeded by the tide-induced bed shear-stress, τ_C (Eq. 1), and by the wave-induced bed shear-stress, τ_W (Eq. 2), considered separately. Porter-Smith et al. (2004), Li et al. (2015), Coughlan et al. (2021) have used this type of representation to regionalise the prevailing processes. The classification scheme used in Porter-Smith et al. (2004) for the Australian Shelf was adapted in this work and a region is categorised as:

- "tide-dominated" when the percentage of time of tidal mobilisation is greater than three times that of wave mobilisation,
- "wave-dominated" when the percentage of time of wave mobilisation is greater than three times that of tidal mobilisation,
- "mixed" in between.

Another useful indicator of sediment mobility is the Mobilisation Frequency Index (MFI), defined as the percentage of time the threshold bed shear-stress for the chosen grain size, τ_{cr}, is exceeded by the maximum bed shear-stress under combined wave and current action, τ_{max} (Eq. 4). MFI therefore gives some indication on how often the seabed sediment is mobilised at a given location.

This is complemented by the Sediment Mobilisation Index (SMI) that integrates both the magnitude and frequency of sediment mobilisation. SMI is calculated as the mean ratio of the maximum combined bed shear-stress, τ_{max}, by the threshold bed shear-stress, τ_{cr} (only for those times when the threshold of motion is exceeded) times the percentage time exceedance (Li et al. 2009).

The spatial distribution of these indices over the study area was computed from the validated numerical model output for 2020-2021. Considering complete years removes any seasonal bias, although it is recognised that a more robust approach would consist in using a longer period (computational time constraints).

3.8 Sediment transport mechanism

The Rouse number, P, is a non-dimensional parameter that defines the shape of the suspended sediment concentration profile. By extension it is often used as an indicator for the mechanism of sediment transport. Bedload transport is prevailing when P values are greater than 2.5, and suspended transport is prevailing when P values are under 1.2 (Fredsøe & Deigaard 1992).

The Rouse number is expressed as the ratio between the sediment settling velocity w_s and the upwards velocity acting on the grain:

$$P = w_s / (\kappa \, u_*) \quad (6)$$

with κ the von Kármán constant = 0.40 (Soulsby 1997), and u_* the friction velocity. In these calculations, w_s. is estimated from Soulsby (1997) in the absence of in-situ measurements, and u_* was replaced by $\sqrt{\tau_m / \rho}$ since wave action will contribute to seabed sediment mobilisation in the study area.

4 RESULTS AND DISCUSSIONS

4.1 Maps of sediment mobility

By computing the percentage time of exceedance of the threshold shear-stress, a spatial assessment of the relative importance of current and wave processes in mobilising seabed sediment was carried out. The result of this analysis is shown in Figure 5. It follows that sediment in the study area is

predominantly mobilised by the strong tidal current (at least three times more than by waves) in relatively deep waters. Over the sand banks (an area broadly delineated by the -15 m MSL contour) the role of waves in stirring the sediments is enhanced and these areas are designated as “mixed” in accordance with Porter-Smith et al. (2004) classification. This corroborates our working hypothesis that wave action should not be discarded as a mechanism for sediment mobilisation (Durand et al. 2022b). Wave-dominated disturbance occurs in very localised areas, only close to the shore, where tidal currents are weakened, and wave orbital velocities stronger owing to reduced water depths. With this scheme, tile #1 is classified as “tide-dominated”.

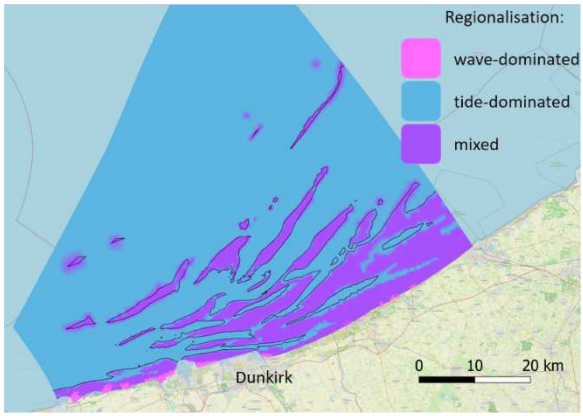

Figure 5. Regionalisation of seabed mobilisation by different dominant processes, also showing the -15 m MSL isobath. (Source of the background data: https://www.openstreetmap.org/).

It is recognised that this regionalisation is the result of an average over a two-year period and does not mean to say that wave contribution to sediment mobilisation is minimal in “tide-dominated” areas. Indeed, during storms for example, the wave action can be stronger than that of the currents in stirring the seabed sediment as illustrated in Durand et al. (2022b).

Figure 6 presents a map of the percentage time exceedance of the threshold bed shear-stress. MFI values range from 0 to 96%. High levels of exceedance (> 70%) are largely correlated to sand bank crests (water depths shallower than 15 m) and the “mixed” disturbance areas highlighted in Figure 5. Within tile #1, the seabed sediment is mobilised 60% of the time on average, with higher rates (up to 67%) on top of the dune crests, in the navigation channel.

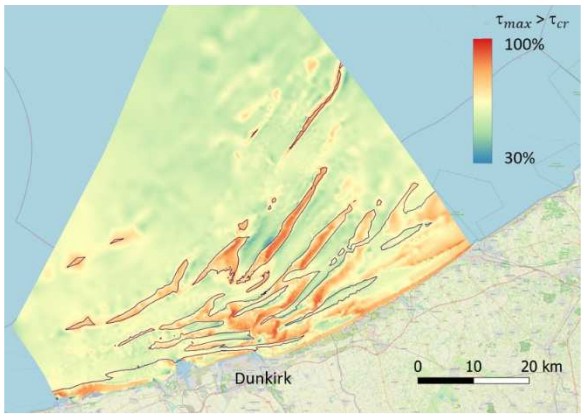

Figure 6. Mobilisation Frequency Index (MFI) computed from two years of model results, also showing the -15 m MSL isobath. (Source of the background data: https://www.openstreetmap.org/).

Figure 7 presents the spatial distribution of the Sediment Mobilisation Index. SMI values typically range between 0 and 2.5 in ’tide-dominated” areas. These values are comparable to those reported by Coughlan et al. (2021) in the Irish Sea, and generally higher than those reported by Li et al. (2015) in the Bay of Fundy. Higher SMI values (typically reaching 5.0) are computed in “mixed” areas, in particular along the coast and atop the sand banks (associated reduced water depths). These values are indicative of intense sediment mobilisation due to the combined wave and current action.

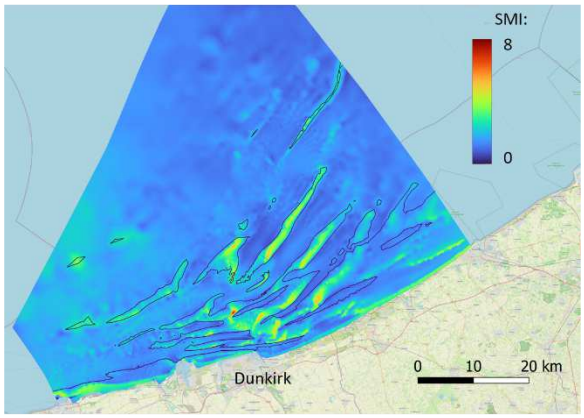

Figure 7. Sediment Mobilisation Index (SMI) computed from two years of model results, also showing the -15 m MSL isobath. (Source of the background data: https://www.openstreetmap.org/).

Within tile #1, SMI values range between 1.2 and 2.0. Remembering that the seabed sediment there is mobilised ca. 60% of the time, the threshold of motion is exceeded between 2 and 3 times, on average over a two-year period. It can be expected that tile #1 be more active during storms.

4.2 Map of sediment transport mechanism

The Rouse number, computed from Equation 6 over the whole model area, and averaged over the two-year period between 2020 and 2021, was estimated in excess of 2.5. This gives some indication that bedload is the dominant sediment transport mechanism in the study area (Fredsøe & Deigaard 1992) and is in line with Borsje et al. (2014) findings on the Dutch continental shelf that marine dunes could only form when Rouse numbers were greater than 2.0.

4.3 Dune profiles in tile #1

The evolution in time of the dune profile along section a'-a" (Figure 2), extracted from the local survey data, is depicted in Figure 8. For clarity, the time intervals between the successive bathymetric surveys will be referred to as periods A to G in the following.

It is clear from Figure 8 that the dunes evolution is not constant in time and is rather dependent on external factors. The dunes are very mobile during period A (compare to C and F with similar durations). In that period, the shape of the dunes remains mostly unchanged, and they migrate ca. 15 m to the East. Interestingly, lee slopes of the dunes become gentler during periods B and G, resulting in an apparent migration of the crest towards the West.

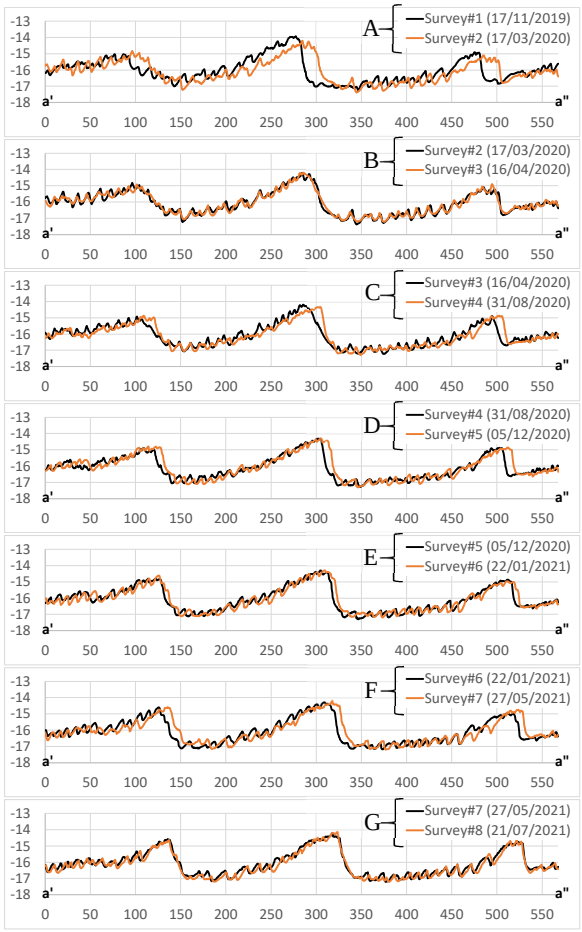

Figure 8. Dune profiles in tile #1, along section a'-a", showing the evolution in time.

5 CONCLUDING REMARKS

A coastal area model is being developed based on the complex process-based open source TELEMAC system. Overall, the comparisons presented in this and earlier work indicate a good performance of the hydrodynamic and wave models in the study area under a range of tidal currents and offshore wave and wind conditions.

Sediment mobility maps have been produced for the study area from validated model (hydrodynamic and wave) data for 2020-2021. The maps indicate that tidal as well as wave action plays a role in mobilising the seabed sediment, the predominant mode of transport being then bedload transport, in line with the presence of marine dunes in the area. The seabed sediment is more frequently set in motion, and bed shear-stresses more largely exceeded, in shallow areas (notably over the sand banks) than in waters deeper than ca. 15 m MSL, in line with expectations.

Focusing on tile #1, the next step will be to quantify how the oceanographic parameters vary between bathymetric surveys to explain the different dynamics illustrated in Figure 8. This task will be performed by including the sediment transport module GAIA (Tassi et al. 2023) into the coastal area model. Preliminary analysis indicates that the wave climate was markedly

different between period A (unusually high proportion of wave heights exceeding 1 m and maybe importantly a high proportion of south-westerly waves) and periods B and G (unusually large proportion of northerly waves) for example.

6 ACKNOWLEDGEMENTS

This work was initiated by France Energies Marines, with financial support from the French National Research Agency ANR (Grant no ANR-10-IEED-0006-34). The authors would like to thank the partners of the MODULLES project for providing site-specific data and giving permission to publish this work.

7 REFERENCES

Ashley, G.M., 1990. Classification of large-scale subaqueous bedforms: A new look at an old problem. Journal of Sedimentary Research 60, 160-172. doi:10.2110/JSR.60.160

Benoit, M., Marcos, F., and Becq, F., 1996. Development of a third-generation shallow water wave model with unstructured spatial meshing. Proceedings 25th Int. Conf. on Coastal Eng. 465-478. doi:10.9753/icce.v25.%25p

Borsje, B., Kranenburg, W., Roos, P., Matthieu, J., and Hulscher, S., 2014. The role of suspended load transport in the occurrence of tidal sand waves. Journal of geophysical research. Earth surface, 119(4), 701-716. doi:10.1002/2013JF002828

Boutier, F., 2007. Arome, avenir de la prévision régionale. La Météorologie, 58, 12-20. doi:10.4267/2042/18203

Coughlan, M., Guerrini, M., Creane, S., O'Shea, M., Ward, S. L., Van Landeghem, K. J., Murphy, J., and Doherty, P., 2021. A new seabed mobility index for the irish sea: Modelling seabed shear stress and classifying sediment mobilisation to help predict erosion, deposition, and sediment distribution. Continental Shelf Research, 229. doi:10.1016/j.csr.2021.104574

Durand, N., Tassi, P., Blanpain, O., and Lefebvre, A., 2022a. Towards numerical modelling of marine dunes in a shallow shelf sea. Actes des XVIIèmes Journées Nationales Génie Côtier-Génie Civil, Chatou, France. in press

Durand, N., Tassi, P., Blanpain, O., and Lefebvre, A., 2022b. Hydrodynamic modelling as a first step to assess marine dune dynamics: influence of waves. XVIIIth Telemac-Mascaret User conference. October 18-19, 2022. Paris-Saclay, France. in press

Fredsøe, J., and Deigaard, R., 1992. Mechanics of Coastal Sediment Transport. World Scientific. doi:10.1142/1546

Hervouet, J.-M., 2007. Hydrodynamics of Free Surface Flows: Modelling with the Finite Element Method. Wiley

Li, M.Z., Zou, Q., Hannah, C., Perrie, W., Prescott, R., and Toulany, B., 2009. Numerical Modelling of Seabed Disturbance and Sediment Mobility with applications to Morphodynamics on the Storm-dominated Sable Island Bank, Scotian Shelf. Geological Survey of Canada, Open File 6155

Li, M.Z., Hannah, C.G., Perrie, W.A., Tang, C.C.L., Prescott, R.H., and Greenberg, D.A., 2015. Modelling seabed shear stress, sediment mobility, and sediment transport in the Bay of Fundy. Can. J. Earth Sci. 52, 757-775. doi:10.1139/cjes-2014-0211

Porter-Smith, R., Harris, P., Andersen, O., Coleman, R., Greenslade, D., and Jenkins, C., 2004. Classification of the australian continental shelf based on predicted sediment threshold exceedance from tidal currents and swell waves. Marine Geology, 211(1), 1-20. doi:10.1016/ j.margeo.2004.05.031

Raoult, C., Joly, A., Andreevsky, M., and Joly-Laugel A., 2018. ANEMOC-3: Improving the ANEMOC-2 Sea state database by adding tide effects. Actes des 16èmes Journées de l'Hydrodynamique, 27-29 Novembre 2018, Marseille, France

Shom, 2015. MNT bathymétrique de façade atlantique. doi:10.17183/MNT_ATL100m_ HOMONIM_WGS84

Soulsby, R., 1997. Dynamics of marine sands. Thomas Telford Publishing

Sutherland, J., Walstra, D.J.R., Chesher, T.J., van Rijn, L.C., and Southgate, H.N., 2004. Evaluation of coastal area modelling systems at an estuary mouth. Coastal Engineering, 51, 119-142. doi:10.1016/j.coastaleng.2003.12.003

Swart, D. H., 1976. Predictive equations regarding coastal transports. Proceedings 15th Int. Conf. on Coastal Eng. 1113–1132. doi:10.9753/icce.v15.65

Tassi, P., Benson, T., Delinares, M., Fontaine, J., Huybrechts, N., Kopmann, R., Pavan, S., Pham, C.T., Taccone, F., and Walther, R., 2023. GAIA - a unified framework for sediment transport and bed evolution in rivers, coastal seas and transitional waters in the TELEMAC-MASCARET modelling system. Environmental Modelling and Software. 159(5). doi:10.1016/j.envsoft.2022.105544

Teles, M., Weiss, M, .and Benoit, M., 2022. Assessment of the ANEMOC-3 sea state hindcast database for modelling a series of energetic winter storms along the French coast. Actes des XVIIèmes Journées Nationales Génie Côtier-Génie Civil, Chatou, France. in press